

REPORT DOCUMENTATION PAGE

AFRL-SR-AR-TR-06-0093

Public reporting burden for this collection of information is estimated to average 1 hour per response, including the time for reviewing instructions, searching existing data sources, gathering and maintaining the data needed, and completing and reviewing this collection of information. Send comments regarding this burden estimate or any other aspect of this collection of information, including suggestions for reducing this burden to Washington Headquarters Services, Directorate for Information Operations and Reports, 1215 Jefferson Davis Highway, Suite 1204, Arlington, VA 22202-4302, and to the Office of Management and Budget, Paperwork Reduction Project (0704-0188), Washington, DC 20503.

1. AGENCY USE ONLY (Leave blank)		2. REPORT DATE 23 March 2006	3. REPORT TYPE AND DATES COVERED Final Report 15 Jan 2003-31 Dec 2005	
4. TITLE AND SUBTITLE Development and Applications of Nanowire Nanophotonics			5. FUNDING NUMBERS G F49620-03-1-0063	
6. AUTHOR(S) Charles. M. Lieber				
7. PERFORMING ORGANIZATION NAME(S) AND ADDRESS(ES) President and Fellows of Harvard College Office for Sponsored Programs 1350 Massachusetts Avenue Cambridge, MA 02138			8. PERFORMING ORGANIZATION REPORT NUMBER	
9. SPONSORING / MONITORING AGENCY NAME(S) AND ADDRESS(ES) Air Force Office of Scientific Research 875 North Randolph St Suite 325, Room 3112 Arlington, VA 22203 <i>Maj. Jennifer Gresham/NL</i>			10. SPONSORING / MONITORING AGENCY REPORT NUMBER	
11. SUPPLEMENTARY NOTES				
12a. DISTRIBUTION / AVAILABILITY STATEMENT Approved for Public Release; distribution is unlimited.				12b. DISTRIBUTION CODE
13. ABSTRACT (Maximum 200 Words) The controlled and predictable synthesis of nanowires and nanowire heterostructures that serve as the basic nanoscale building blocks for photonic devices has been carried out. Nanocluster catalyzed growth was used to prepare gallium nitride based nanowire materials, including radial nanowire heterostructures in which the composition and/or doping was modulated perpendicular to the axis of a nanowire. Scanning electron microscopy and transmission electron microscopy were used to characterize the detailed structure and composition of nanowires down to the atomic level, and demonstrate that desired nanowire structure could be made in a controlled manner. In addition, the critical optical and optoelectronic properties of the nanowire and nanowire heterostructure building blocks, and their behavior as photonic device elements, including nanoscale light-emitting diodes, lasers and avalanche photodiodes were characterized. Photoluminescence studies showed that at the single nanowire level that nanowires exhibit emission colors that were tuned specifically by the composition of the nanowires. Nanolithography was also used to make electrical contacts to nanowire structures and use combined optical microscopy and electrical transport measurements to demonstrate the successful demonstration of the first multi-color nanoscale light-emitting diodes, the first nanowire electrical injection laser, and the first nanowire avalanche photodiode detector.				
14. SUBJECT TERMS nanowires; nanophotonics; light emitting diodes; avalanche detectors				15. NUMBER OF PAGES 34
				16. PRICE CODE
17. SECURITY CLASSIFICATION OF REPORT	18. SECURITY CLASSIFICATION OF THIS PAGE	19. SECURITY CLASSIFICATION OF ABSTRACT	20. LIMITATION OF ABSTRACT	

**Final Technical Report for
GRANT NUMBER F49620-03-1-0063
15 January 2003 – 31 December 2005**

Table of Contents

I. Report Documentation Page	1
II. Technical Report	
A) Executive Summary	3
B) Comprehensive Technical Summary.....	3
C) Personnel Involved in Research Effort.....	22
D) Ph.D. Theses Stemming from Research Effort.....	22
E) Publications Stemming from Research Effort.....	22
F) Presentations Stemming from Research Effort.....	25
G) Technology Transitions Stemming from Research Effort.....	32
H) Honors and Awards Earned During the Award Period.....	33

II. TECHNICAL REPORT

A. EXECUTIVE SUMMARY

The overall objectives of our AFOSR funded research program are to develop semiconductor nanowires as building blocks for nanoscale photonic devices, and to exploit these new photonic devices in fundamental studies relevant to the AFOSR and DoD, including sensing, lithography and imaging. To achieve these objectives we are pursuing a research path defined by the bottom-up assembly paradigm for systems development, which focuses on (i) controlled synthesis of nanoscale building blocks, (ii) characterization of fundamental physical properties of the building blocks, and (iii) assembly of building blocks into functional devices and systems. First, we will develop methods for the controlled and predictable synthesis of nanowires and nanowire heterostructures that will serve as the basic nanoscale building blocks for photonic devices. Nanocluster catalyzed growth will be used to develop the synthesis of gallium nitride and alloys of this material to provide building blocks for photonic devices that can span the ultraviolet through visible regions of the electromagnetic spectrum. We will also use nanocluster catalyzed growth to investigate the synthesis of axial nanowire heterostructures in which the composition and/or doping are modulated along the axis of a nanowire in a controlled manner, and we will explore the growth of core-shell and core-multi-shell nanowire heterostructures in which the composition and/or doping are modulated radially in a controlled manner. Second, we will investigate the optical and electrical properties of these new nanowire and nanowire heterostructure building blocks to define their fundamental and unique characteristics and potential photonic applications. Our optical and electrical studies will focus on measurements at single nanowire level to provide information about intrinsic properties without ensemble broadening. Lastly, directed assembly and nanofabrication methods will be used to prepare nanowire-based photonic structures, such as multi-color nanoscale light-emitting diodes and nanowire laser sources, and optical and electrical measurements will be used to define the characteristics of these novel nanophotonic devices.

B. COMPREHENSIVE TECHNICAL SUMMARY

This research program is centered on developing semiconductor nanowires as building blocks for nanoscale photonic devices and photonic systems, and subsequently exploiting these new photonic devices in critical AFOSR and DoD applications, including imaging, sensing, information processing, and nanoscale lithography. To achieve these objectives we are pursuing a research path defined by the bottom-up paradigm for nanosystems, which focuses on (i) controlled synthesis of nanoscale building blocks, (ii) characterization of fundamental physical properties of the building blocks, and (iii) assembly of building blocks into functional devices and systems. Within this overall program framework, several significant accomplishments have been made since the start of this new program. We have demonstrated that nanoscale light-emitting diodes with colors spanning from the ultraviolet to near-infrared region of the electromagnetic spectrum can be prepared using a solution-based approach in which emissive electron-doped semiconductor nanowires are assembled with nonemissive hole-

doped silicon nanowires in a crossed nanowire architecture, where the colors are specified in a predictable way by the band-gaps of the group III-V and II-VI nanowire building blocks. We have shown that this approach can be extended to combine nanoscale electronic and photonic devices into integrated structures, where a nanoscale transistor is used to switch the nanoLED on and off. We have demonstrated that this approach can be generalized to hybrid devices consisting of nanowire emitters assembled on lithographically patterned planar silicon structures, thereby providing a route for integrating photonic devices with conventional silicon microelectronics. We have shown that nanoLEDs can optically-excite emissive molecules and nanoclusters, and hence can enable a range of integrated sensor/detection ‘chips’ with multiplexed analysis capabilities. We have developed a new and general strategy for efficient injection of carriers in active nanophotonic devices involving the synthesis of well-defined doped core/shell/shell (CSS) nanowire heterostructures. We have enabled this concept through the growth n-GaN/InGaN/p-GaN CSS nanowire structures by metal-organic chemical vapor deposition, and used detailed electron microscopy studies to reveal that the CSS nanowires are defect-free single crystalline structures with shell thickness and composition well controlled during synthesis. We have demonstrated that the GaN/InGaN/p-GaN CSS heterostructures emit blue light in photoluminescence measurements, and moreover, that photonic devices fabricated using these building blocks emit intense blue light under electrical injection. We have developed an approach for guiding and manipulating light on sub-wavelength scales using active nanowire waveguides and devices, and have used quantitative studies of cadmium sulfide nanowire structures to demonstrate that light propagation takes place with only moderate losses through sharp and even acute angle bends. We have shown that the transmission through nanowire waveguides can be efficiently modulated using electric fields, thereby demonstrating for the first time an nanoscale electro-optic modulator with capability of manipulating photons for optical processing. We have demonstrated the first nanoscale avalanche photodiode detector, which was developed from a crossed nanowire architecture, and have shown that this device can amplify signal a million times, and detect 10’s of photons with sub-wavelength spatial resolution. We have demonstrated that the nanowire avalanche photodetectors can be assembled into arrays and thus open up unique opportunities for high-gain and high-spatial resolution optical detection. Therefore, these results demonstrate that our program represents an attractive approach for building nanophotonic devices and systems critical to AFOSR and DoD needs.

Multicolor crossed nanowire nanophotonic sources. Our approach to nanoscale photonic devices is based upon sequential deposition of p-type and n-type NW materials into a crossed NW architecture using directed fluidic assembly (Fig. 1a), where the cross points are electrically addressable. In the crossed NW p-n structure, the n-type NW is chosen to be a direct band-gap semiconductor with efficient light emission and the p-type material is silicon, which has an indirect band-gap and inefficient light emission (Fig. 1b). The crossed NW heterostructures can be described qualitatively by a staggered type-II band diagram (Fig. 1b), and will emit light characteristic of the n-type NW element when the applied forward bias voltage exceeds the band-gap/e; the indirect gap SiNW is a passive optical component and used for its well-defined electronic properties. Important

features of the crossed NW nanoLED concept, include (i) the emitted colors are limited only by the available direct gap NW building blocks, (ii) the active device area is of nanometer dimensions making these point light sources, (iii) the crossed NW architecture enables the formation of single and multicolor arrays and integration of photonic and nanoelectronic elements, and (iv) the nanophotonic devices can be assembled on both rigid and flexible substrates.

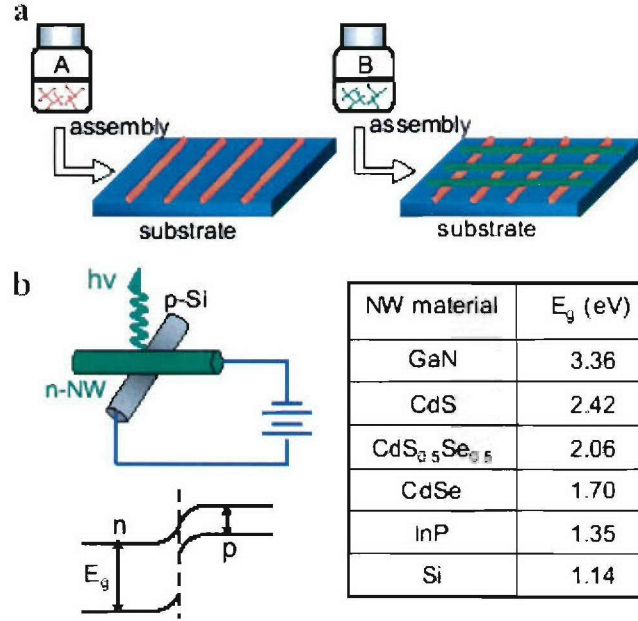


Figure 1. a) Schematic of crossed NW heterojunctions assembly. First, a parallel array of A NWs (orange lines) is aligned on the substrate with fluidic assembly method, and then a second parallel array of B NWs (green lines) is orthogonally to achieve a crossed NW matrix. b) Top-left and low-left schematics show a nanoLED structure formed between p-SiNW and a direct band gap n-type NW and its corresponding band diagram. The table lists band gaps of different materials (at 300 K) used in this study.

The NW building blocks used in these studies, including direct band gap III-V (e.g., GaN and InP) and II-VI (e.g., CdS and CdSe) materials, have been prepared as single crystal by metal nanocluster catalyzed growth. The bulk band-gaps of these semiconductors enable light emission from ultraviolet (UV, GaN) to near infrared (NIR, InP) as confirmed for individual NWs using photoluminescence measurements. Electrical transport measurements made on individual NWs in a FET geometry showed that the GaN, CdS, CdSSe, CdSe and InP NWs are all n-type with room-temperature electron mobilities, $100\text{-}5000\text{ cm}^2/\text{V}\cdot\text{s}$, that are comparable to bulk materials. Previous studies in our group have demonstrated that boron-doped p-type SiNWs exhibit carrier mobilities comparable to or better than bulk material.

Current-voltage (I-V) data for a typical p-Si/n-GaN crossed NW junction (Fig. 2a) shows well-defined current rectification expected for a p-n diode with a turn-on voltage of ca. 1 V. These data are consistent with previous studies of n-GaN/p-Si diodes used as

nanoelectronic logic gates. Notably, applying a forward bias to the p-n junction yields strong electroluminescence (EL) at room temperature (Fig. 2b). The EL spectrum shows a peak maximum at ca. 365 nm consistent with GaN band edge emission, and demonstrates that crossed NW devices can function as UV nanoLEDs. Studies of over 30 n-GaN/p-Si nanoLEDs yielded similar I-V and EL results. Data plotted for four representative devices (Fig. 2c) show several important points. First, light emission is detected when the bias voltage exceeds ca. 3.5 V. This threshold is consistent with the 3.36 eV band gap of GaN, which when exceeded, leads to radiative recombination of electron/hole pairs in GaN.^[20] Second, the emission intensity increases rapidly with voltage and exhibits a nearly linear dependence on current above the threshold. The estimated quantum efficiency (electron to photon) is ca. 0.1%. This efficiency is less than commercial LEDs, although could be improved by passivating surface traps and using a larger band-gap p-type NW for hole injection. Third, stable (≥ 1 hour) UV output is observed in air at room temperature at drive currents of ca. 2 μ A. Lastly, the near-field optical power densities, which are estimated 50 nm from a typical UV nanoLED, are on the order of 100 W/cm². Notably, this value exceeds that needed in a number of optical applications, including lithography and spectroscopy.

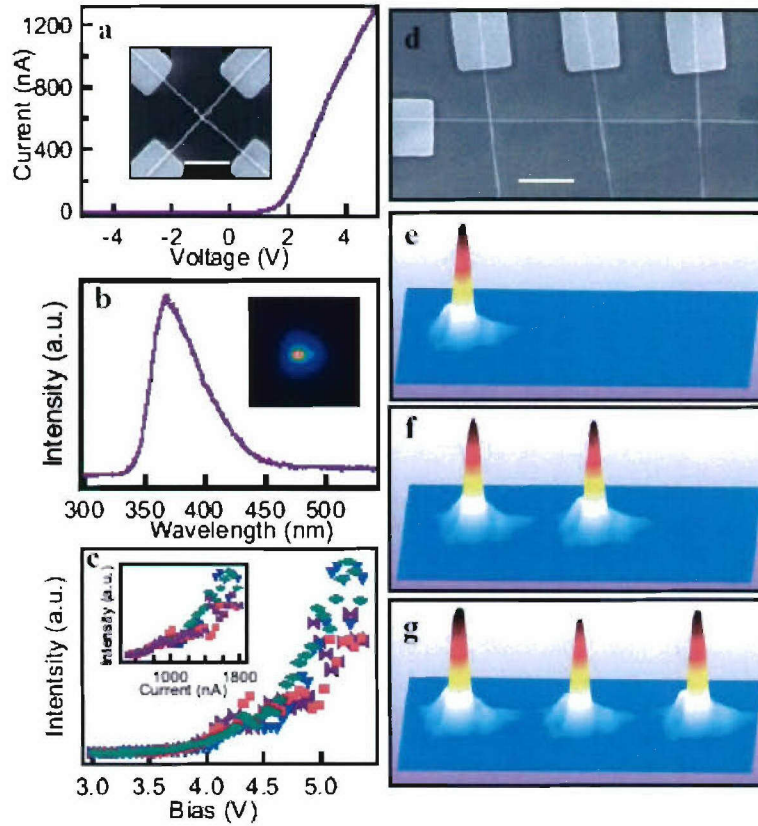


Figure 2. a) I-V data recorded for a p-Si/n-GaN crossed NW junction. (inset) scanning electron microscopy (SEM) image of a typical cross junction. Scale bar 1 μ m. b) EL spectrum from the crossed p-Si/n-GaN NW nanoLED with peak at \sim 365 nm. (inset) EL image showing spatial map of the intensity with maximum at the NW cross point. c) Emission intensity vs. forward bias voltage for four distinct nanoLEDs. (inset) Emission

intensity vs. injection current relation for the same four nanoLEDs. d) Representative SEM image of 3 p-n diodes formed by crossing three p-Si NWs over an n-GaN NW; scale bar is 2 μm . (e-f) Three dimensional EL intensity plots of the three p-n diodes as a bias of 5.5 V is added sequentially to each Si NW with the GaN NW at ground.

The reproducibility and stability of the n-GaN/p-Si nanoLEDs suggests that they could be assembled into addressable arrays. To test this idea we used fluidic assembly to make three junctions consisting of a n-GaN NW and three crossed p-Si NWs (Fig. 2d). Transport measurements show that each of the three nanoscale junctions form independently addressable p-n diodes with clear current rectification. These p-n diodes each function as UV nanoLEDs, where each source can be individually switched on or off. Figures 2e-g show a sequence of EL images where the three nanoLEDs were sequentially turned on, and demonstrate that the output intensity is similar for three sources. We believe these array results highlight the potential of the bottom-up approach for assembling integrated photonic devices, and should be important in exploiting such nanoLEDs in applications where parallel writing (e.g., lithography and information storage) and spectroscopy (e.g., integrated sensors) could be advantageous.

In addition, we assembled p-n junctions using p-Si NWs and a variety of other n-type NW materials, including CdS, CdSeS, CdSe and InP, to test whether our approach could yield nanoLEDs with a broad range of outputs. Transport measurements show that these p-n diodes behave similarly to that of p-Si/n-GaN p-n diode. For example, I-V data recorded from a p-Si/n-CdS junction shows clear current rectification (inset, Fig. 3a). When the CdS-Si NW diode forward bias voltage exceeds ca. 2.6 V, strong light emission from the cross point is observed at room temperature. The emission maximum at ca. 510 nm, corresponds to CdS band-edge emission. Significantly, the light emission is so strong that it can be readily imaged with a color CCD camera and is visible to the bare eye in a dark room. The quantum efficiency of the CdS nanoLED device is estimated to be 0.1-1%, which is significantly higher than previously reported InP NIR ($\sim 0.001\%$) and GaN (above) nanoLEDs. The enhanced quantum efficiency may be explained in part by the intrinsically low surface state density for II-VI materials. Moreover, studies of nanoLEDs based on CdSSe, CdSe and InP NWs showed EL peak maxima and images characteristic of band edge emission from the crossed junctions made with these materials: CdS_{0.5}Se_{0.5}, 600 nm; CdSe, 700nm; and InP, 820nm (Fig. 3a).

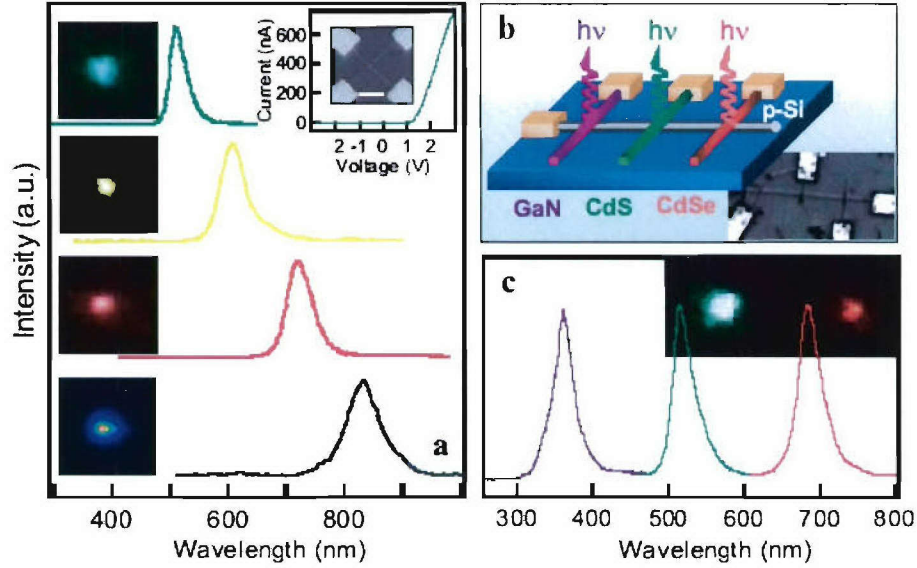


Figure 3. a) EL spectra from crossed p-n diodes of p-Si and n-CdS, CdSSe, CdSe and InP, respectively (top to bottom). Insets at left are corresponding EL images for CdS, CdSSe and CdSe (color CCD), and InP (liquid-nitrogen cooled CCD) nanoLEDs. The top, right inset shows representative I-V and SEM data recorded for a p-Si NW/n-CdS crossed NW junction; scale bar 1 μm . Spectra and images were collected at +5 V. b) Schematic and corresponding SEM image of a tricolor nanoLED array. The array was obtained by fluidic assembly and photolithography with ca. 5 μm separation between NW emitters. c) Normalized EL spectra and color images from the three elements.

We have exploited the ability to form nanoLEDs with nonemissive SiNW hole-injectors to assemble multicolor arrays consisting of n-type GaN, CdS and CdSe NWs crossing a single p-type SiNW (Fig. 3b). Normalized emission spectra recorded from the array demonstrates three spatially and spectrally distinct peaks with maxima at 365, 510, and 690 nm (Fig. 3c) consistent with band edge emission from GaN, CdS and CdSe, respectively. In addition, color images of EL from the array shows the green and red emission from p-Si/n-CdS p-Si/n-CdSe crosses, respectively (inset, Fig. 3c). The ability to assemble different materials and independently tune the emission from each nanoLED offers substantial potential producing specific wavelength sources, and demonstrates an important step towards integrated nanoscale photonic circuits.

Optoelectronic circuits. In addition, we have assembled optoelectronic circuits consisting of integrated crossed NW LED and FET elements (Fig. 4a). Specifically, one GaN NW forms a p-n diode with the SiNW and a second GaN NW functions as a local gate as described previously. Measurements of current and emission intensity versus gate voltage (Fig. 4b) show that (i) the current decreases rapidly with increasing voltage as expected for a depletion mode FET, and (ii) the intensity of emitted light also decreases with increasing gate voltage. When the gate voltage is increased from 0 to +2 V, the current is reduced from ca. 2200 nA to an off state, where the supply voltage is -6 V. Advantages of this integrated approach include switching with much smaller changes in voltage (0 to 2 vs. 0 to 6 V) and the potential for much more rapidly switching. The

ability use the nanoscale FET to switch reversibly the nanoLED on and off is shown clearly in Figure 4c.

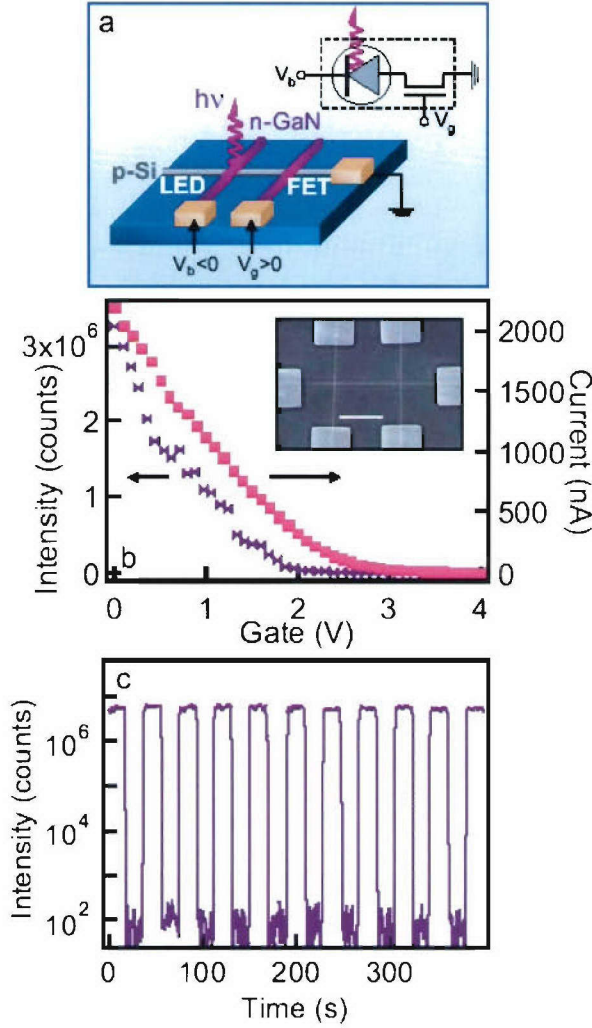


Figure 4. a) Schematic of an integrated crossed NW FET and LED. Inset shows the equivalent circuit. b) Plots of current and emission intensity of the nanoLED as a function of voltage applied to the NW gate at a fixed bias of -6 V. (inset) SEM image of a representative device; scale bar, 3 μ m. c) EL intensity vs. time relation a voltage applied to NW gate is switched between 0 and +4 V for fixed bias of -6 V.

Hybrid bottom-up/top-down photonic structures. We have also investigated the potential of coupling the bottom-up assembly of nanophotonic devices described above together with top-down fabricated silicon structures, since this could provide a new approach for introducing efficient photonic capabilities into integrated silicon electronics. We implemented this hybrid top-down/ bottom-up approach by (1) using lithography to pattern p-type silicon wires on the surface of a silicon-on-insulator (SOI) substrate, and then (2) assembling n-type emissive NWs on top of silicon structures to form arrays consisting of p-n junctions at cross points (Fig. 5a). Conceptually, this hybrid structure

(Fig. 5b) is virtually the same as the crossed NW structures described above and should produce EL in forward bias. Notably, I-V data recorded for a hybrid p-n diode formed between the p-Si and a n-CdS NW show clear current rectification (Fig. 5c) and sharp EL spectrum peaked at 510 nm (Fig. 5d), which is consistent with CdS band edge emission. To explore the reproducibility of this new hybrid approach we have also characterized arrays. For example, a 1×7 crossed array consisting of a single CdS NW over 7-fabricated p-Si wires (Fig. 5e) exhibits well-defined emission from each of the cross points in the array (Fig. 5f). Similar results were obtained for two-dimensional arrays, and demonstrate clearly that bottom-up assembly has the potential to introduce photonic function into integrated silicon microelectronics.

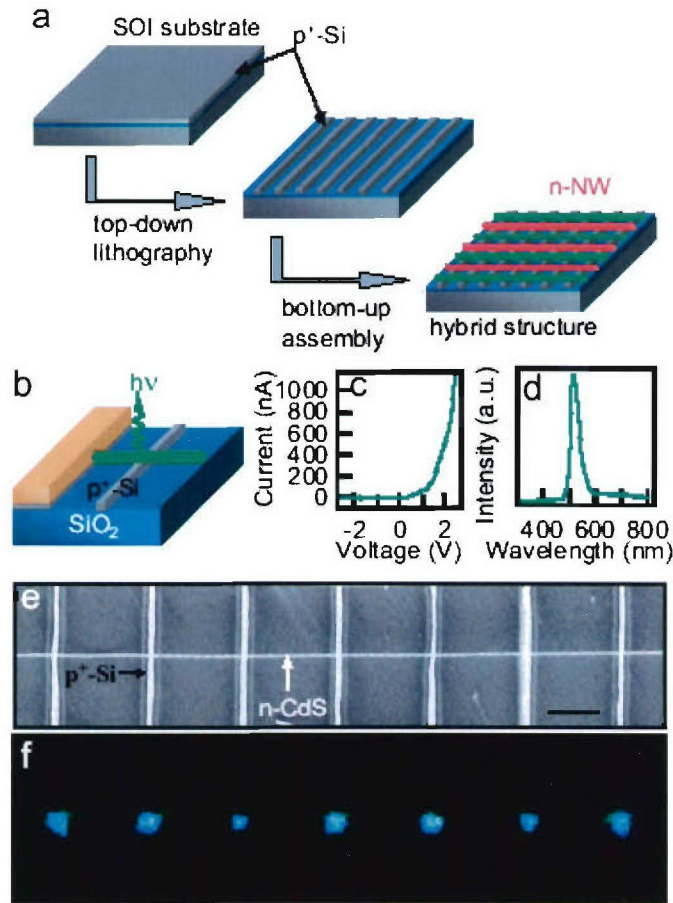


Figure 5. a) Schematic illustrating fabrication of hybrid structures. A silicon-on-insulator (SOI) substrate is patterned by standard electron-beam or photolithography followed by reactive ion etching. Emissive NWs are then aligned on to patterned SOI substrate to form photonic sources. b) Schematic of a single LED fabricated by the method outlined in (a). c) I-V behavior for a crossed p-n junction formed between a fabricated p^+ -Si electrode and an n-CdS NW. d) EL spectrum from the forward biased junction. e) SEM image of a CdS NW assembled over seven p^+ -silicon electrodes on a SOI wafer; scale bar is 3 μ m. f) EL image recorded from an array consisting of a CdS NW crossing seven p^+ -Si electrodes. The image was acquired with +5 V applied to each silicon electrodes while the CdS NW was grounded.

Nanophotonic sources for integrated sensors. The localized EL from crossed NW nanoLEDs and hybrid LEDs can result in a near-field power densities greater than 100 W/cm^2 , which is sufficient to excite molecular and nanoparticle chromophores. To explore this important possibility we use a CdS-based nanoLED to excite and record the emission spectra from CdSe quantum dots (QDs) and propidium iodide (a fluorescent nucleic acid stain) (Fig. 6). Notably, the emission of CdSe QDs and propidium iodide obtained by nanoLED excitation show essentially the same spectra (solid lines, Figs. 6a,b) as those obtained using much larger conventional excitation source (dashed lines, Figs. 6a,b) (see Experimental). These results demonstrate that nanoLEDs could function as excitation sources for integrated chemical and biological analysis.

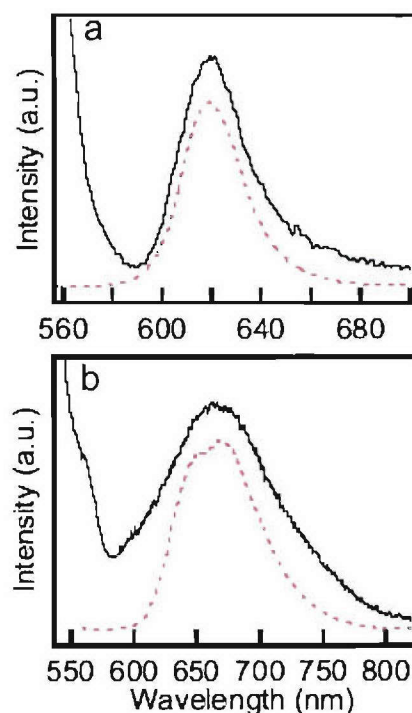


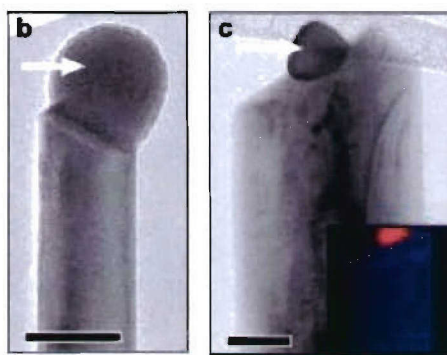
Figure 6. a) Solid line is the emission spectrum recorded from CdSe QDs excited using a p-Si/n-CdS NW nanoLED; the QD emission maximum was 619 nm. The increasing intensity on the shorter wavelength side of the emission peak corresponds to the tail of the CdS nanoLED. Dashed red line is the spectrum of pure CdSe QDs excited using an Ar-ion laser. b) Solid line is the emission spectrum from propidium iodide excited using a p-Si/n-CdS NW nanoLED. Dashed red line is emission spectrum of propidium iodide obtained in aqueous solution (Fluorolog, ISA/Jobin Yvon-Spex).

MOCVD growth core/shell GaN-based nanowire building blocks. We have also installed a state-of-the-art MOCVD reactor for the controlled growth of Al-Ga-In nitride based nanowires with controlled composition and doping. We have focused on GaN-based materials since alloys of (Al-Ga-In)N are direct band gap semiconductors with

potential for light emission from the ultraviolet through visible regions of the electromagnetic spectrum. Previous studies of planar LEDs have shown that n-GaN/InGaN/p-GaN and related double heterostructures exhibit enhanced light emission efficiency compared to simple n-GaN/p-GaN diode structures, and thus suggest that CSS versus core/shell (CS) structures would be ideal candidates for GaN-based active nanowire devices. The nanowire CSS structures also have potentially significant differences compared to planar heterostructures beyond that of dimensionality. In particular, because nanowire synthesis is essentially substrate-free it should prevent formation of dislocations originating from lattice mismatch between GaN and growth substrates, and thereby reduce nonradiative recombination (at these defects) relative to planar structures.

Our approach for preparing the GaN-based CSS structures involves initial metal nanocluster mediated vapor-liquid-solid (VLS) growth of an n-type GaN core followed by sequential radial growth of intrinsic InGaN and p-type GaN shells. Scanning electron microscopy (SEM) images of Si-doped GaN nanowires obtained following axial elongation reveal a high yield of uniform nanowire cores and transmission electron microscopy (TEM) images (Fig. 7) show that the

Figure 7. (b) Bright-field TEM image of n-GaN nanowire core demonstrating that the diameter is the same as the corresponding nanocluster. (c) Bright-field TEM image of n-GaN/InGaN CS nanowire; the white arrow highlights the nanocluster. Inset: EDX map of nickel (red) and gallium (blue) for this same nanowire. Scale bars are 50 nm.

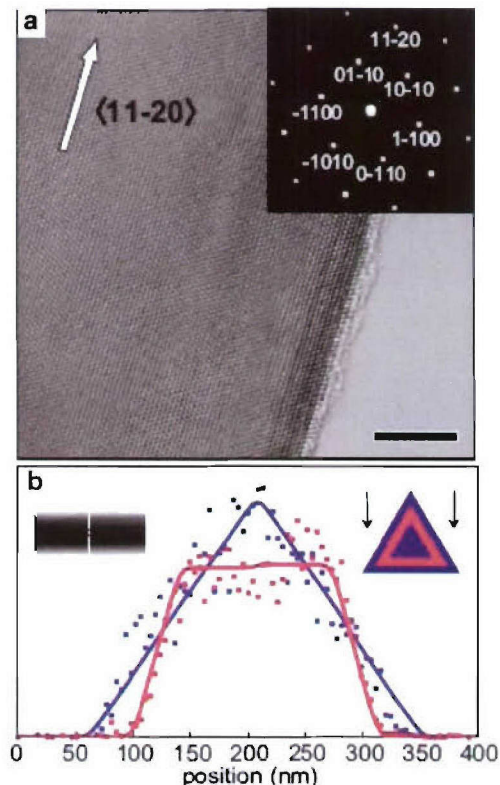


nanowire diameter is essentially the same as the nickel nanocluster diameter as expected for the VLS process. Corresponding TEM images of n-GaN/InGaN CS nanowires demonstrate that the overall diameters increase following InGaN shell growth. Examination of a representative CS nanowire end (Fig. 7) shows that the overall diameter is substantially larger than that of the nanocluster, in contrast to the core nanowires, and that the nanowire has a triangular cross-section. Energy dispersive X-ray spectroscopy (EDX) mapping also demonstrates that nanoclusters at the CS nanowire ends are nickel while the larger core-shell nanowire structure contains Ga, In and N. Taken together, these results show our capability for growing these new structures.

High-resolution TEM and EDX were used to characterize in greater detail the CS and CSS nanowires. Lattice-resolved images obtained from n-GaN/InGaN/p-GaN CSS nanowires containing a nominal 20% In in the InGaN shell (Fig. 8) demonstrate that the CSS nanowires have a single crystalline structure, while lower resolution bright-field images show no evidence of either dislocations or other defects following growth of the inner InGaN and outer p-GaN shells; these results imply that strain at the GaN/InGaN interface is not relaxed. To characterize the CS and CSS nanowires further we recorded

and analyzed EDX compositional line profiles. Overall, the EDX data shows clearly distinct differences in the spatial profiles of In and Ga that are qualitatively consistent with well-defined InGaN shells in the CS and CSS structures. In addition, quantitative analysis show that shell thickness and tilt angle obtained from the fit are in

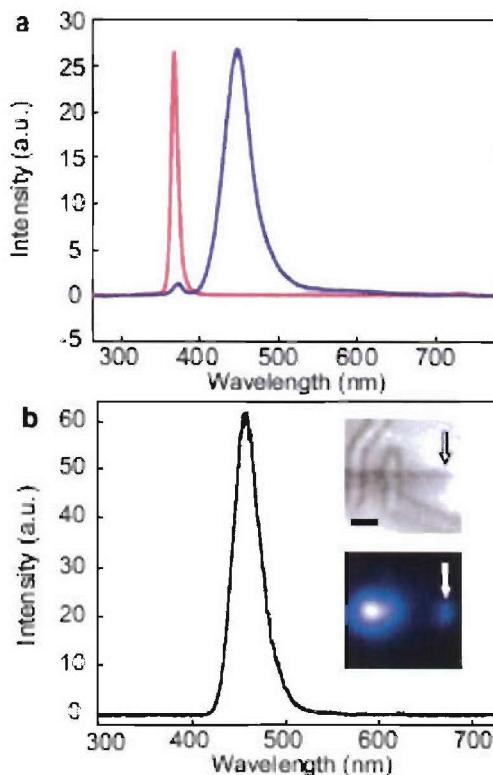
Figure 8. Crystalline structure and composition profiles of n-GaN/InGaN CS and n-GaN/InGaN/p-GaN CSS nanowires. (a) High-resolution TEM image of single crystalline n-GaN/InGaN/p-GaN CSS nanowire taken along the [0001] zone axis. The white arrow highlights the $\langle 11-20 \rangle$ growth direction for the CSS nanowire. Scale bar is 5 nm. Inset: corresponding electron diffraction pattern indexed for the [0001] zone axis. (b) Normalized EDX line profiles for gallium (blue symbols) and indium (red symbols) recorded on an n-GaN/InGaN/p-GaN CSS nanowire. Insets: scanning TEM images of the nanowires, and models for the nanowire cross-sections (blue and red regions represent GaN and InGaN, respectively).



good agreement with the thickness estimated from the onset of the In signal (after the outer GaN shell) and the orientation angle determined from images, respectively. Taken together these TEM and EDX studies provide demonstrate clearly our ability to grow single crystal GaN/InGaN CS and GaN/InGaN/GaN CSS nanowire heterostructures with well-defined and controllable shell thicknesses and composition.

Fundamental optical and opto-electronic properties of core/shell GaN-based nanowire building blocks. We have also characterized the GaN-based CSS nanowires further by optical, electrical and optoelectronic measurements. Photoluminescence (PL) spectra recorded on n-GaN and n-GaN/InGaN/p-GaN CSS nanowire structures (Fig. 9) demonstrate that emission is

Figure 9. Optoelectronic properties of n-GaN/InGaN/p-GaN CSS nanowires. (a) Normalized PL spectra obtained from single n-GaN (red) and n-GaN/InGaN/p-GaN CSS (blue) nanowire. (b) EL spectrum recorded from a forward-biased CSS p-n junction at 7 V. Insets: bright field (upper) and EL (lower) images of a CSS structures. The EL image was recorded at 4 K with a forward bias of 12 V. White arrows in both images highlight the end of the CSS nanowire. Scale bar is 2 μm .



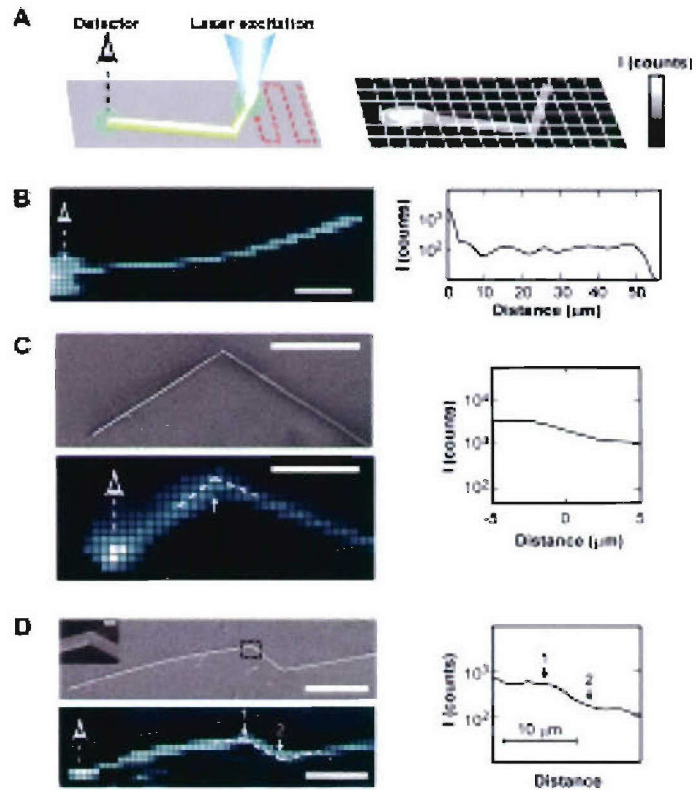
band-edge from GaN. The position, sharpness and absence of longer wavelength emission demonstrate the excellent crystalline quality of the n-GaN core. Significantly, the PL spectra obtained from n-GaN/InGaN/p-GaN CSS structures show a dominant emission peak at 448 nm. This wavelength is consistent with band-edge emission from an InGaN structure of composition $\text{In}_{0.18}\text{Ga}_{0.82}\text{N}$. The InGaN emission is ca. 20 times stronger than the small GaN band-edge emission peak also present in the PL spectrum, which shows that the much smaller volume InGaN shell in our CSS structures provides an efficient region for radiative recombination.

The n-GaN/InGaN/p-GaN CSS nanowire heterostructures have been used to prepare functional nanoscale LEDs. Electrical transport measurements made in a field-effect transistor configuration demonstrate that the Si-doped GaN nanowires and the Mg-doped GaN outer shells of the CSS nanowires are n-type and p-type, respectively. These results are consistent with our previous studies of homogeneous n- and p-type nanowires, and planar materials. Simultaneous electrical contacts to both the n-type core and p-type outer shell of individual CSS nanowires, which are required to inject electrons and holes into the InGaN quantum well, were achieved using a focused ion beam microscope to etch and expose selectively the core at one end of the CSS nanowires. Current versus voltage data recorded between contacts to the n-type core and p-type shell show current rectification with a sharp onset at ca. 4 V in forward bias that is characteristic of a p-n diode. Notably, the electroluminescence (EL) spectrum collected from a representative forward biased n-GaN/InGaN/p-GaN CSS nanowire device (above) exhibits an intense peak at 456 nm with a FWHM of 50 nm. These values are in good agreement with the PL spectra recorded from similar CSS nanowires. In addition, no emission is observed at the

GaN band edge or longer wavelengths associated with defect or impurity states. These results show that injected electrons and holes recombine in an $\text{In}_{0.18}\text{Ga}_{0.82}\text{N}$ active shell in these new nanowire heterostructures. The EL observed at the end of the CSS structure also shows that these nanowires can serve as optical waveguides, can function as the optical cavity needed for single nanowire injection lasers.

Nanowire photonic circuit elements: active waveguides. To evaluate the potential of active nanowire waveguides we have quantitatively characterized losses through straight and sharply bent sub-wavelength diameter CdS nanowire structures using scanning optical microscopy (SOM). In these experiments, spatial maps of the intensity of light emitted from the end of a nanowire are recorded as a function of the position of a diffraction-limited laser spot as shown in Figure 10. The SOM images recorded from a nearly straight nanowires exhibit little

Figure 10. (A) Scheme for SOM imaging. The intensity at the end indicated by the detector is plotted on a color scale as a function of laser position to generate SOM images. (B) SOM image and intensity map of a single CdS nanowire; the reference end is indicated with detector. The scale bar is 10 μm . (C) SEM and corresponding SOM image. The scale bars in both images are 10 μm . At right, intensity profile along the path indicated in the SOM image. (D) SEM of the nanowire structure and corresponding SOM image. Scale bars, 10 μm . At right, intensity profile along the path indicated in the SOM map. Arrows 1 and 2 designate the locations of the two intra-nanowire bends.

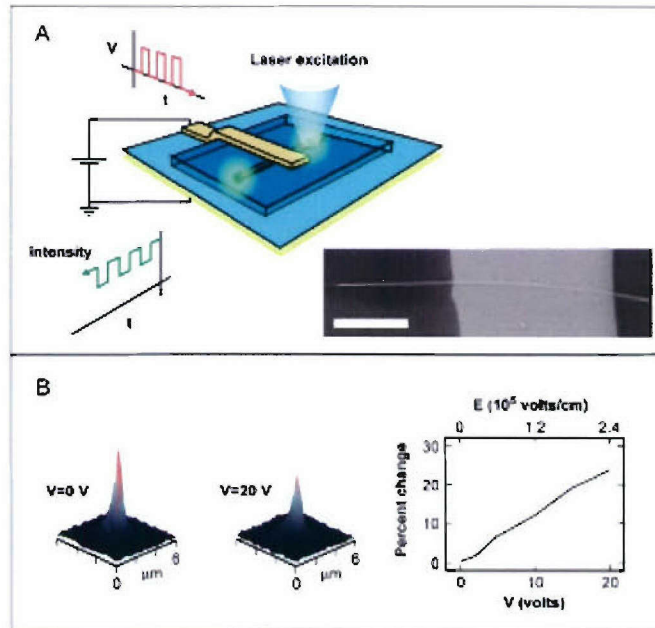


intensity variation as a function of detector-laser excitation source separation along the wire, which is indicative of a good waveguide. A plot of intensity vs. position quantitatively shows that there is no loss within the limits of our measurement. Significantly, we have also used SOM to that the optical loss is small across sharp bends in CdS nanowire with a bend formed by a change in axial growth direction. The radius of curvature for such abrupt bends is not well-defined, although the radius of the nanowire,

100 nm, provides an upper bound and highlights the sub-wavelength nature of these waveguides and bends. Analysis of the intensity vs. position along the nanowire shows that the loss through this abrupt bend is 1-2 dB. In addition, SOM characterization of a ca. 55 μm long nanowire containing two abrupt $46 \pm 1^\circ$ bends separated by ca. 6 μm in a Z-type structure demonstrates that it is possible to guide light through multiple sub-wavelength bends with only a moderate loss. Our results compare well to a similar double bend structure with a ca. 1.5 μm wide waveguide channel fabricated in a photonic crystal, and thus have shown clearly the promise of this discovery.

Nanowire photonic circuit elements: manipulating light at the nanoscale. In addition, the combination of active nanowire waveguides with electrical inputs has been demonstrated. For example, we have demonstrated the first modulation of light transmission through a nanowire waveguide subject to a time varying electric field as shown in Figure 11. Voltage-dependent

Figure 11. Electrical modulation of light in nanowire waveguides. (A) Schematic of a nanowire EOM. A cw laser source injects light into the nanowire waveguide, and a variable electric field applied across the nanowire using a parallel-plate capacitor geometry modulates the end intensity. Inset, SEM image of a typical device; scale bar is 5 μm . (B) Intensity modulation at the nanowire end. At left, images of the end spot for voltages of 0 and 20 V. At right, the change in output intensity as a function of applied voltage; the corresponding electric field (calculated from the electrode separation) is shown on the top axis.

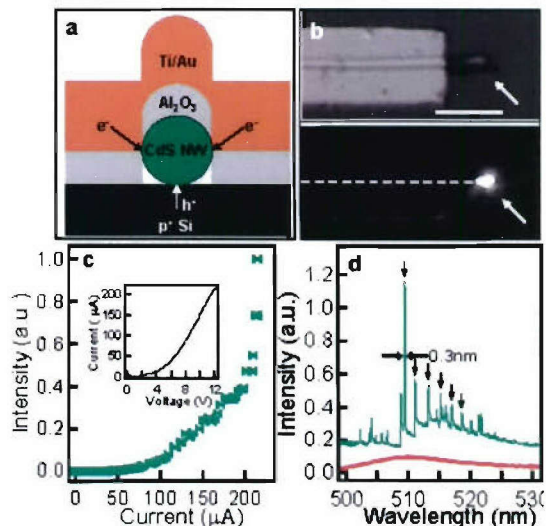


measurements show a linear decrease up to 20 V; although deviations from linearity are observed at larger voltages an attenuation of -3 dB is achieved at 60 V. Studies of devices made with smaller (150 vs. 700 nm) electrode separations further confirm that the percentage modulation scales with the electric field (not capacitor voltage). Notably, comparison of our devices to recently reported Si-based and InGaAs waveguide modulators shows that the unoptimized nanowire device performance is substantially better than or comparable to more conventional integrated structures: 1 dB/10 μm , nanowire; 0.015 dB/10 μm , Si; and 2.3 dB/10 μm , InGaAs, where all are measured with 10 V modulation voltage. Integrated modulators, which are important in many photonic

systems, have not yet been reported for 2D photonic crystals but our work suggests that they can be readily combined with nanowire photonic components.

Demonstration of electrically-driven nanowire laser. We have recently described the first example of electrically-driven lasing from individual nanowires. Optical and electrical measurements made on single crystal cadmium sulfide nanowires showed that these structures can function as Fabry-Perot optical cavities with mode spacing inversely related to the nanowire length. To investigate nanowire injection lasers we have implemented a hybrid structure (Fig. 12a) in which the n-type CdS nanowire laser cavities are assembled onto p-Si electrodes defined in heavily p-doped planar substrates. This structure produces the n-CdS/p-Si heterojunction needed for an injection device. An image of a typical device is shown in Fig. 12b. Current vs. voltage data recorded from devices fabricated in this way show current rectification with a forward bias turn-on of 2-5 V (inset, Fig. 12c), which is consistent with the formation of p-n diodes. The variation in turn-on voltage is believed to be due to Al_2O_3 barrier between the metal/CdS contact and/or oxide at the CdS/p-Si junction.

Figure 12. Nanowire electrical injection laser. (a) Schematic showing the cross section of the device structure. (b), Optical and electroluminescence images recorded from this device at room-temperature with an injection current of ca. 80 μA . The arrow highlights emission from the CdS nanowire end. (c) Emission intensity vs. injection current. (d) Electroluminescence spectra obtained from the nanowire end with injection currents of 120 μA (red) and 210 μA (green). The black arrows highlight Fabry-Perot cavity modes with an average spacing of 1.83 nm.



Images of the room-temperature electroluminescence produced in forward bias from these hybrid structures (Fig. 12b) exhibit strong emission from the exposed CdS nanowire ends. Measurements of the nanowire end electroluminescence intensity vs. current (Fig. 12c) show an initial increase in the intensity at ca. 90 μA and then a much more rapid and highly nonlinear increase at ca. 200 μA . Significantly, at low injection currents the spectrum of the end emission (Fig. 12d) shows a broad peak with FWHM ~ 18 nm consistent with spontaneous emission, but above the ca. 200 μA threshold the spectrum quickly collapsed into a limited number of very sharp peaks with a dominant emission line at 509.6 nm (Fig. 12d). The dominant mode has an instrument resolution limited line width of only 0.3 nm. Taken together these observations provide strong evidence for lasing from single nanowire injection structures at room temperature.

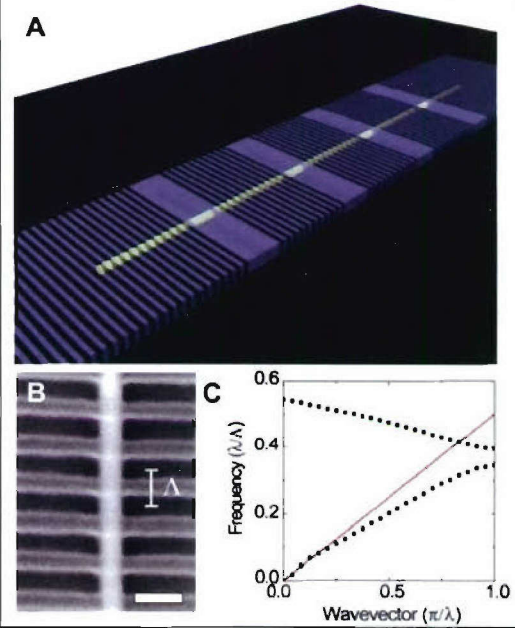
Our results show that nanoscale injection lasers can be made from single semiconductor nanowires, and represent a new and powerful approach for producing integrated electrically-driven photonic devices. This basic approach, which relies upon

bottom-up assembly of the key laser cavity/medium in a single step, can be extended to other materials, such as GaN and InP nanowires, to produce nanoscale lasers that not only cover the ultraviolet through near infrared spectral regions but also can be integrated as single or multi-color laser source arrays in silicon microelectronics and lab-on-a-chip devices. There are also scientific and technical challenges that may need to be addressed to realize this potential, including the development of more efficient cavities and injection schemes. We believe that both issues could be addressed at the nanowire growth stage prior to device assembly by preparing Bragg gratings at the nanowire ends through axial composition modulation, and using core-shell nanowire structures to enable uniform injection into the active medium/cavity, respectively. By addressing these and other issues, such as quantifying contributions to optical losses within the nanowire cavity, nanowire lasers could be developed into systems that impact a number of areas where solid state lasers are used today, including telecommunications and data storage, and may enable new applications in highly integrated chemical/biological sensors, near-field optical lithography, a host of scanning probe microscopies, and perhaps even laser-based surgery with unprecedented resolution.

Hybrid nanowire photonic crystal and microresonator structures. Hybrid structures that merge nanowire building blocks with top-down fabricated elements could offer a solution to this fundamental issue of coupling light into and out of nanowires as well as enabling other opportunities. We have recently reported the first studies of light-matter interaction between single semiconductor nanowires and lithographically defined cavities. We demonstrated that photonic crystal structures can be used to suppress and control spatially the emission from specific regions of a nanowire, and moreover, we show that nanowires can be coupled to microresonators yielding efficient feedback and amplified spontaneous emission.

Our basic hybrid structure consists of a free-standing CdS nanowire core embedded in a 1-dimensional (1D) photonic crystal, where the photonic crystal can be fabricated as a uniform periodic grating or containing specifically-designed defects as illustrated schematically in Figure 13A. A representative scanning electron microscopy (SEM) image of the periodic region of a hybrid structure is shown in Figure 13B. This image shows that the photonic crystal can be well-aligned relative to the individual, embedded nanowire.

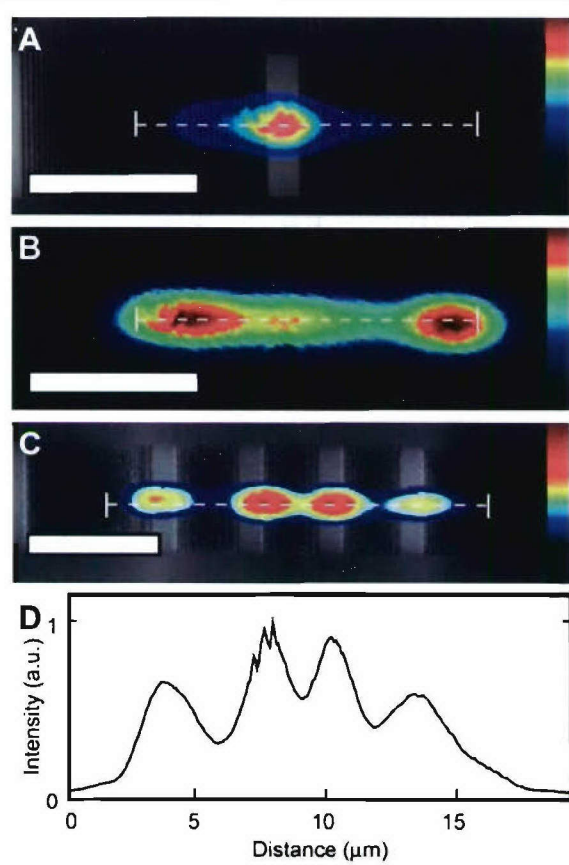
Figure 13. Nanowire photonic crystal structure and modeling. (A) Schematic of the nanowire photonic crystal with four engineered defects. (B) SEM image of a nanowire photonic crystal with a periodicity, $\Lambda = 190\text{nm}$. Scale bar, 200 nm. (C) Dispersion diagram calculated by FDTD simulation showing the presence of a photonic band gap. Red line is the light line in air.



Finite-difference time-domain (FDTD) simulations were used to determine the photonic band gap for the hybrid nanowire 1D photonic crystal structures. We evaluated different hybrid structures in order to achieve a good overlap of the photonic band gap with the electronic band gap of the CdS nanowire, 2.5 eV at 300 K. The calculated dispersion diagram for a 90 nm diameter CdS nanowire and 190 nm period 1D photonic crystal (Figure 13C) shows that the photonic crystal behaves as a grating acting strongly on the evanescent field. Specifically, a wide photonic band gap exists in which light propagation along the wire is suppressed. The calculated photonic band gap, $477 < \lambda < 544$ nm, spans the entire emission range of high-quality CdS nanowires, which exhibit an emission peak and full-width at half-maximum of 515 and 15 nm, respectively.

The effect of the photonic band gap on the nanowire photonic crystal hybrid structures was first investigated by introducing one or more PMMA defects in the periodic 1D structure as illustrated schematically in Figure 13A. A typical photoluminescence (PL) image recorded from a CdS nanowire photonic crystal structure with a single defect consisting of the removal of 5 grating periods is shown in Figure 14A. This PL image, which is overlaid with a registered atomic-force microscopy (AFM) image of the hybrid structure, demonstrates clearly localized radiation from the artificial defect and inhibition of emission along the nanowire photonic crystal axis, including the nanowire ends. Control experiments involving the deposition of PMMA onto the photonic crystal structures (Figure 14B), which fills in the air gaps and removes the grating, were also carried out to address the effects of electron beam exposure during fabrication. Notably, these PL images show that localized emission is eliminated and conventional nanowire end emission is observed (Figure 14B). Taken together, these data show that the hybrid nanowire photonic crystal structures can spatially control emission from nanowires through the introduction of defects.

Figure 14. Analysis of nanowire photonic crystal structures containing engineered defects. (A) PL image (false color) superimposed on the AFM image (grayscale) of a nanowire photonic crystal with one defect. Dotted line indicates the nanowire position. Scale bar, 5 μm . (B) PL image of the same nanowire after filling in the photonic crystal structure with PMMA. Scale bar, 5 μm . (C) PL image (false color) superimposed on the AFM image (grayscale) of a nanowire photonic crystal containing four defects, which are visible as vertical lighter gray stripes. Scale bar, 5 μm . (D) Line scan through the PL image in (C) taken along the nanowire axis. The periodicity of the 1D grating regions in (A) and (C) was 180 nm.



To further explore this concept we have fabricated and studied the optical properties of hybrid structures with multiple defects introduced in the photonic crystal lattice. For example, a PL image of a structure with four defects is shown in Figure 14C. These data, which are registered to the corresponding AFM image of the hybrid structure, and the line-scan in Figure 2D demonstrate localized emission specifically from the four defect sites. In addition, PL spectroscopy studies of the localized emission did not exhibit additional peaks in the CdS emission spectrum. These results suggest that either the cavity mode associated with the defect has a low quality factor or that there is no cavity mode within the emission energy range. While future simulations and experiments will be needed to address further these possibilities, we note that these studies demonstrate for the first time that localized emission is a robust effect in nanowire photonic crystals with engineered defects.

The generality of our approach for creating hybrid nanowire photonic systems was further explored by fabricating nanowire racetrack microresonator structures. In contrast to 1D photonic crystal cavities based on distributed feedback, nanowire microresonators trap light by total internal reflection, which provides resonant recirculation. An optical micrograph of a representative hybrid structure (Figure 15A) shows the racetrack microresonator defined in PMMA¹³ with a 2 μm track width and a 11.2 μm long, 200nm diameter CdS nanowire embedded in one arm. The total optical length of the resonator, taking into account the refractive indices of PMMA and CdS, is approximately 130 μm .

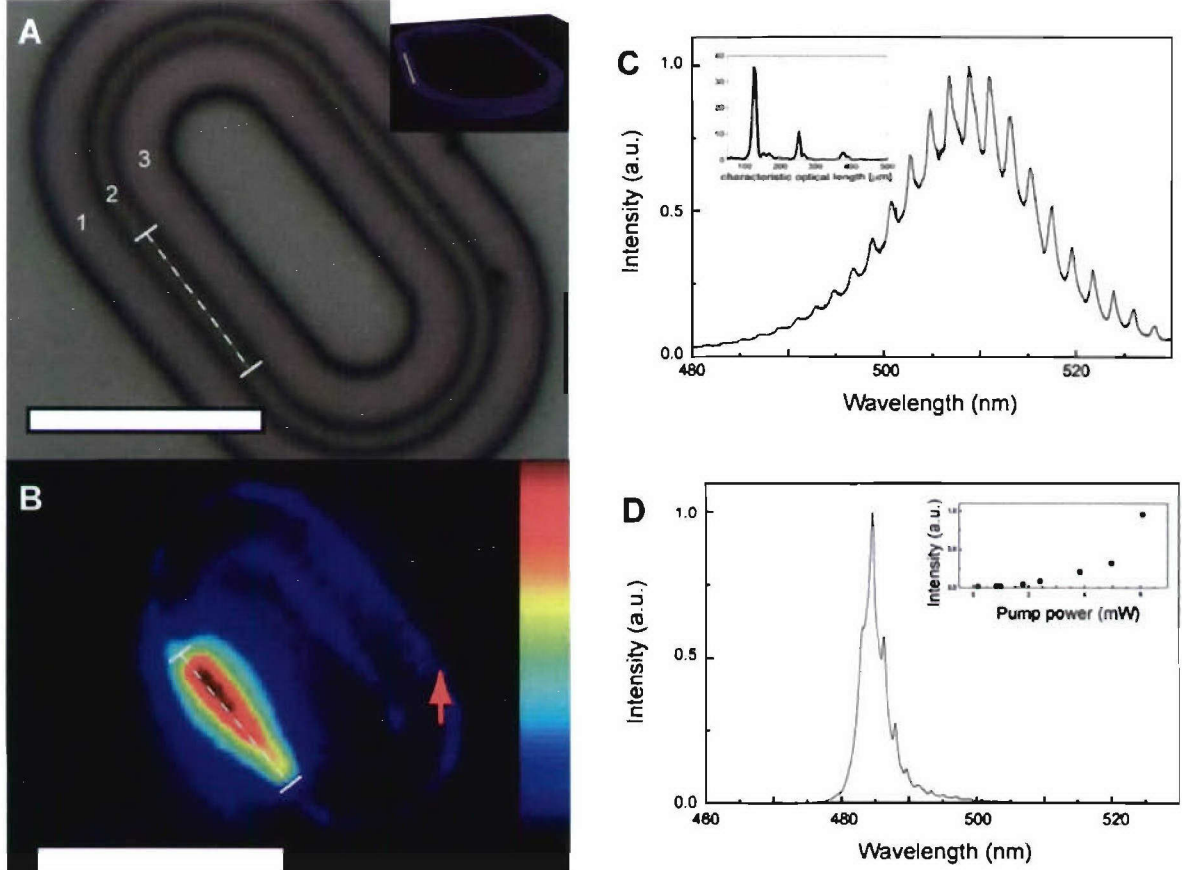


Figure 15. Nanowire racetrack microresonator. (A) White-light optical image of the nanowire/microresonator structure, where regions 1 and 3 correspond to the air surrounding the PMMA racetrack, region 2. The dashed line indicates the nanowire position. Inset, 3D model of the nanowire racetrack microresonator. (B) PL image of the nanowire microresonator. The red arrow indicates the region over which spectra were collected and the dashed line corresponds to position of nanowire as in (A). Both scale bars, 20 μm . (C) PL spectrum recorded at room-temperature at location indicated in (B). Inset, Fourier-transform of the PL spectrum. (D) PL Spectrum at ca. 4 K. Inset, peak output power versus incident pump power.

PL images recorded from the hybrid structure (Figure 15B) show strong emission at the position of the nanowire and also exhibit emission at the edges of the opposite arm of the resonator. These results show that light emitted by the nanowire is guided by total internal reflection around the racetrack microresonator. A representative PL spectrum recorded from the hybrid structure remote to the position of the embedded nanowire is shown in Figure 15C. This spectrum exhibits a progression of relatively sharp, periodic peaks on top of the typical CdS emission that correspond to cavity modes. Last, we have measured the input/output power dependence at low temperatures, and significantly, found that the excitation power dependence (inset, Figure 15D) showed a superlinear increase in the output emission intensity as a function of incident laser power with an exponent of 2.9. The superlinear increase in the emission output power and the

emergence of a dominant mode from the relatively broad spectrum are consistent with amplified stimulated emission from the hybrid structure. We believe that further refinement of the nanowire/microresonator hybrid structures (e.g., reducing the optical losses of the racetrack resonator) has the potential to generate low-threshold external cavity nanowire lasers with the fabricated racetrack enabling a number of options beyond that possible with the nanowire alone.

C. PERSONNEL INVOLVED IN RESEARCH EFFORT

Charles M. Lieber, Principal Investigator
Linda Ross, Laboratory Administrator
Ritesh Agarwal, Post Doctoral Fellow
Silvija Gradecak, Post Doctoral Fellow
Yat Li, Post Doctoral Fellow
Paul Ashby, Graduate Student, Ph.D. received 5/03.
Fang Qian, Graduate Student, current.
Yue Wu, Graduate Student, current.

D. PH.D THESES STEMMING FROM RESEARCH EFFORT

Fang Qian, "Gallium Nitride Heterostructures for Nanophotonics"

E. PUBLICATIONS STEMMING FROM RESEARCH EFFORT REFEREED JOURNAL ARTICLES AND BOOK CHAPTERS:

X. Duan, Y. Huang, R. Agarwal and C.M. Lieber, "Single-Nanowire Electrically Driven Lasers," *Nature* **421**, 241-245 (2003).

X. Duan, Y. Huang and C.M. Lieber, "Nanowire Nanocircuits," in *2003 McGraw-Hill Yearbook of Science and Technology*, E. Geller, J. Weil, D. Blumel, A. Rappaport, (Eds.), 272-276 (McGraw Hill, 2003).

Z. Zhong, F. Qian, D. Wang and C.M. Lieber, "Synthesis of p-Type Gallium Nitride Nanowires for Electronic and Photonic Nanodevices," *Nano Lett.* **3**, 343-346 (2003).

D. Wang and C.M. Lieber, "Inorganic Materials: Nanocrystals Branch Out," *Nature Mater.* **2**, 355-356 (2003).

X. Duan, Y. Huang, Y. Cui and C.M. Lieber, "Nanowire Nanoelectronics Assembled from the Bottom-Up" in *Molecular Nanoelectronics*, M. A. Reed and T. Lee (Eds.) 199-227 (American Scientific Publishers, 2003).

C.M. Lieber, "Nanoscale Science and Technology: Building a Big Future from Small Things," *MRS Bull.* **28**, 486-491 (2003).

- C.J. Barrelet, Y. Wu, D.C. Bell and C.M. Lieber, "Synthesis of CdS and ZnS Nanowires Using Single-Source Molecular Precursors," *J. Am. Chem. Soc.* **125**, 11498-11499 (2003).
- D. Whang, S. Jin, Y. Wu and C.M. Lieber, "Large-Scale Hierarchical Organization of Nanowire Arrays for Integrated Nanosystems," *Nano Lett.* **3**, 1255-1259 (2003).
- Y. Cui, X. Duan, Y. Huang and C.M. Lieber, "Nanowires as Building Blocks for Nanoscale Science and Technology" in *Nanowires and Nanobelts – Materials, Properties and Devices*, Z.L. Wang, ed. 3-68 (Kluwer Academic/Plenum Publishers, 2003).
- M.C. McAlpine, R.S. Friedman, S. Jin, K. Lin, W.U. Wang and C.M. Lieber, "High-Performance Nanowire Electronics and Photonics on Glass and Plastic Substrates," *Nano Lett.* **3**, 1531-1535 (2003).
- Z. Zhong, D. Wang, Y. Cui, M.W. Bockrath and C.M. Lieber, "Nanowire Crossbar Arrays as Address Decoders for Integrated Nanosystems," *Science* **302**, 1377-1379 (2003).
- M.M. Ziegler, C.A. Picconatto, J.C. Ellenbogen, A. DeHon, D. Wang, Z. Zhong and C.M. Lieber, "Scalability Simulations for Nanomemory Systems Integrated on the Molecular Scale," *Ann. N.Y. Acad. Sci.* **1006**, 312-330 (2003).
- Y. Wu, Y. Cui, L. Huynh, C.J. Barrelet, D.C. Bell and C.M. Lieber, "Controlled Growth and Structures of Molecular-Scale Silicon Nanowires," *Nano Lett.* **4**, 433-436 (2004).
- D. Wang, F. Qian, C. Yang, Z. Zhong and C.M. Lieber, "Rational Growth of Branched and Hyperbranched Nanowire Structures," *Nano Lett.* **4**, 871-874 (2004).
- S. Jin, D. Whang, M.C. McAlpine, R.S. Friedman, Y. Wu and C.M. Lieber, "Scalable Interconnection and Integration of Nanowire Devices without Registration," *Nano Lett.* **4**, 915-919 (2004).
- A.B. Greytak, L.J. Lauhon, M.S. Gudiksen and C.M. Lieber, "Growth and transport properties of complementary germanium nanowire field-effect transistors," *Appl. Phys. Lett.* **84**, 4176-4178 (2004).
- Y. Wu, J. Xiang, C. Yang, W. Lu and C.M. Lieber, "Single-crystal metallic nanowires and metal/semiconductor nanowire heterostructures," *Nature* **430**, 61-65 (2004).
- D. Whang, S. Jin and C.M. Lieber, "Large-Scale Hierarchical Organization of Nanowires for Functional Nanosystems," *Japanese J. Appl. Phys.* **43**, 4465-4470 (2004).
- D.C. Bell, Y. Wu, C.J. Barrelet, S. Gradecak, J. Xiang, B.P. Timko and C.M. Lieber, "Imaging and Analysis of Nanowires," *Microsc. Res. Tech.* **64**, 373-389 (2004).
- F. Qian, Y. Li, S. Gradecak, D. Wang, C.J. Barrelet and C.M. Lieber, "Gallium Nitride-Based Nanowire Radial Heterostructures for Nanophotonics," *Nano Lett.* **4**, 1975-1979 (2004).

- C.J. Barrelet, A.B. Greytak and C.M. Lieber, "Nanowire Photonic Circuit Elements," *Nano Lett.* **4**, 1981-1985 (2004).
- G. Zheng, W. Lu, S. Jin and C.M. Lieber, "Synthesis and Fabrication of High-Performance n-Type Silicon Nanowire Transistors," *Adv. Mater.* **16**, 1890-1893 (2004).
- Y. Huang and C.M. Lieber, "Integrated nanoscale electronics and optoelectronics: Exploring nanoscale science and technology through semiconductor nanowires," *Pure Appl. Chem.* **76**, 2051-2068 (2004).
- Y. Huang, X. Duan and C.M. Lieber, "Nanowires for Integrated Multicolor Nanophotonics," *Small* **1**, 142-147 (2005).
- Y. Huang, X. Duan and C.M. Lieber, "Semiconductor Nanowires: Nanoscale Electronics and Optoelectronics," in *Dekker Encyclopedia of Nanoscience and Nanotechnology*, J.A. Schwarz, Ed. (Marcel Dekker, Inc., 2005).
- X. Duan and C.M. Lieber, "Semiconductor Nanowires: Rational Synthesis," in *Dekker Encyclopedia of Nanoscience and Nanotechnology*, J.A. Schwarz, Ed. (Marcel Dekker, Inc., 2005).
- R. Agarwal, C.J. Barrelet and C.M. Lieber, "Lasing in Single Cadmium Sulfide Nanowire Optical Cavities," *Nano Lett.* **5**, 917-920 (2005).
- M.C. McAlpine, R.S. Friedman and C.M. Lieber, "High-Performance Nanowire Electronics and Photonics and Nanoscale Patterning on Flexible Plastic Substrates," *Proc. IEEE* **93**, 1357-1363 (2005).
- P.V. Radovanovic, C.J. Barrelet, S. Gradecak, F. Qian and C.M. Lieber, "General Synthesis of Manganese-Doped II-VI and III-V Semiconductor Nanowires," *Nano Lett.* **5**, 1407-1411 (2005).
- A.B. Greytak, C.J. Barrelet, Y. Li and C.M. Lieber, "Semiconductor nanowire laser and nanowire waveguide electro-optic modulators," *Appl. Phys. Lett.* **87**, 151103 (2005).
- S. Gradecak, F. Qian, Y. Li, H.-G. Park and C.M. Lieber, "GaN nanowire lasers with low lasing thresholds," *Appl. Phys. Lett.* **87**, 173111 (2005).
- R. Agarwal, K. Ladavac, Y. Roichman, G. Yu, C.M. Lieber and D.G. Grier, "Manipulation and assembly of nanowires with holographic optical traps," *Opt. Express* **13**, 8906-8912 (2005).
- F. Qian, S. Gradecak, Y. Li, C. Wen and C.M. Lieber, "Core/Multishell Nanowire Heterostructures as Multicolor, High-Efficiency Light-Emitting Diodes," *Nano Lett.* **5**, 2287-2291 (2005).

C.J. Barrelet, J. Bao, M. Loncar, H.-G. Park, F. Capasso and C.M. Lieber, "Hybrid Single-Nanowire Photonic Crystal and Microresonator Structures," *Nano Lett.* **6**, 11-15 (2006).

F. PRESENTATIONS STEMMING FROM RESEARCH EFFORT

Invited Presentations: C. M. Lieber

February 17, 2003 – Gordon Research Conference on Chemical Reaction at Surfaces, Ventura, CA

"Nanowire Building Blocks for Nanoscale Science and Technology"

March 3, 2003 – American Physical Society Conference, Austin, TX

"James McGroddy Prize Talk - Functional Nanostructured Materials"

March 11, 2003 – Student Selected Speaker in Inorganic Chemistry, University of Illinois at Urbana-Champaign, Champaign, IL

"Nanowires as Building Blocks for Nanoscale Science and Technology"

April 3, 2003 - University of Connecticut RT Major Symposium, Storrs, CT

"Nanowires as Building Blocks for Nanoscience and Nanotechnology"

April 30, 2003 – Columbia University Nanocenter, New York, NY

"Nanowires as Building Blocks for Nanoscience: Building a Big Future From Small Things!"

May 23, 2003 – Georgia Institute of Technology, Atlanta, GA

"Nanoscience: Building a Big Future from Small Things"

July 8, 2003 – Center for Integration of Medicine & Innovative Technology, Boston, MA

"Nanotechnology Meets Biology: From Ultrasensitive Detection of Proteins to Screening Small Molecule-Protein Interactions"

August 4, 2003 – GRC on Clusters, Nanocrystals & Nanostructures, New London, CT

"Nanowires for Nanosensing"

August 7, 2003 – GRC on Chemical Sensors & Interfacial Design, Newport, RI

"Sensing with Nanowires"

August 21, 2003 – Harrison-Howe Award, University of Rochester, NY

"Nanowires as Building Blocks for Nanoscale Science and Technology"

September 4, 2003 – 2003 Nelson W. Taylor Award, Pennsylvania State University, University Park, PA

"Nanoscience and Nanotechnology: Building a Big Future from Small Things"

September 10, 2003 – IBM Zürich Distinguished Lecturer Series, IBM Zürich Research Laboratory, Switzerland

“Nanowires as Building Blocks for Nanoscale Science and Technology”

September 11, 2003 – International Nano Conference 2003, St. Gallen, Switzerland
Plenary Lecture: “Nanowires as Building Blocks for Nanoscale Science and Technology – Building a Big Future from Small Things”

October 23, 2003 – NASA Tech Briefs Nanotech 2003, Cambridge, MA
Keynote Address: “Nanoscience and Nanotechnology: Building a Big Future From Small Things”

November 11, 2003 – 48th Annual Francis Clifford Phillips, Distinguished Lecture, University of Pittsburgh, PA
“Nanowires as Building Blocks for Nanoscale Science and Technology”

November 12, 2003 – 48th Annual Francis Clifford Phillips Lecture Series, University of Pittsburgh, PA

“Nanoscience and the Pathway Towards Nanocomputing”

November 17, 2003 - 2003-2004 Rayson Huang Visiting Lecturer in Chemistry, University of Hong Kong

“Nanowires: Building Blocks for Nanoscale Science and Technology”

November 17, 2003 - 2003-2004 Rayson Huang Visiting Lecturer in Chemistry, University of Hong Kong
“Photonics at the Nanoscale: From Nanowire Building Blocks to Emerging Applications”

November 18, 2003 - 2003-2004 Rayson Huang Visiting Lecturer in Chemistry, University of Hong Kong
“Nanoscience and the Pathway Towards Nanocomputing”

November 19, 2003 – Hong Kong University of Science and Technology
“Nanowires as Building Blocks for Nanoscale Science and Technology”

December 9, 2003 – 2003 International Electron Devices Meeting, Washington, DC
“Nanowires as Building Blocks for Nanoelectronics and Nanophotonics”

January 12, 2004 – DARPA Workshop on the Integration of Scalable CMOS Systems with Novel Nanostructures, McLean VA
“CMOS-Nanowire Hybrids for High-Performance Electronics, Photonics and More”

February 12, 2004 – MITRE Technology Speaker Series, Bedford MA
“Nanowires: Building Blocks for Nanotechnology”

March 8, 2004 – NSTI Nanotech 2004, Boston MA
Keynote: “NANOWIRES: Creating Nanosystems and the Nanotechnology Revolution”

March 29, 2004 – 227th ACS National Meeting (Nanoscience in Inorganic Chemistry), Anaheim CA

“Nanowires as building blocks for nanoscale science and technology”

March 30, 2004 – 227th ACS National Meeting (PChem Award Symposium), Anaheim CA

“Nanowires and nanoscale science: Building toward future technologies”

March 31, 2004 – Applied Biosystems, Inc., Foster City CA

“Nanowires: Building Blocks for Nanotechnology”

April 5, 2004 – 2003-2004 Izaak M. Kolthoff Lectureship, University of Minnesota-Twin Cities

“Nanowires: From Fundamental Science to Functional Systems”

April 6, 2004 – 2003-2004 Izaak M. Kolthoff Lectureship, University of Minnesota-Twin Cities

“Nanoscience and the Pathway to Nanocomputing”

September 14, 2004 - 131st Meeting of the National Cancer Advisory Board:
Nanotechnology Seminar, Bethesda, MD

“Nanoscience for Cancer Biology, Diagnosis & Treatment”

November 18, 2004 – Princeton Physics Colloquium Series, Princeton NJ

“Nanoscience: Physics, Chemistry and Much More”

December 2, 2004 – 24th Army Science Conference, Orlando FL

“Nanowire Nanosensors”

December 7, 2004 – 30th Anniversary of Samsung Electronics Semiconductor Business, Seoul Korea

Keynote: “Nanotechnology: Emerging Opportunities in Electronics and Much More!”

December 14, 2004 – 2004 IEEE International Electron Devices Meeting, San Francisco CA

“Nanowires: Building Blocks for the Assembly of Integrated Nanosystems”

10 February 2005 – 27th Annual Alexander Graham Bell Lecture, McMaster University, Canada

“Nanotechnology: From Biological Sensing to Electronics and Much More!”

22 March 2005 – Second International Workshop on Nano and Bio-Electronics Packaging, Georgia Institute of Technology

Keynote: “Nanowires: From Biological Sensing to Computing and Much More!”

7 April 2005 – 2005 Fritz London Memorial Lecture, Duke University, Durham NC
“Nanotechnology: Emerging Opportunities in Electronics, Biology and Much More!”

5 May 2005 - Samuel McElvain Seminar Series (Materials Chemistry Division),
University of Wisconsin-Madison
“Nanoscience and the Pathway to Nanotechnologies”

16 May 2005 – Gerhard Schmidt Memorial Lecture, Weizmann Institute of Science,
Israel
“Nanoscience & Nanotechnology: Emerging Opportunities in Electronics, Biology and
Much More!”

7 June 2005 – International Symposium on “Chemistry in the Emerging Fields of
Nanotechnology and Biotechnology,” Seoul National University, South Korea
“Nanotechnology: From Fundamental Science to Emerging Opportunities in Electronics,
Biology and Much More!”

8 June 2005 – Samsung SAIT, South Korea
“Nanotechnology: From Fundamental Science to Emerging Opportunities in Electronics,
Biology and Much More!”

9 June 2005 – China NANO 2005, Beijing China
Plenary: “Nanotechnology: Emerging Opportunities in Electronics, Biology and Much
More!”

9 June 2005 – Molecular Science Forum, Chinese Academy of Sciences, China
“Nanowires for Nanoscience and Nanotechnology”

21 June 2005 – 65th Annual Physical Electronics Conference, University of Wisconsin-
Madison
Keynote: “Nanoscience and the Pathway to Nanotechnologies”

29 September 2005 – MESA+ Day Annual Meeting 2005, University of Twente, The
Netherlands
Plenary: “Nanowires for Nanoscience and Nanotechnology”

6 October 2005 – Symposium on Semiconductor Nanowires, Lund University, Sweden
Keynote: “Nanowires, Nanoscience and Emerging Nanotechnologies”

24 October 2005 – Optics East 2005, Boston MA
Keynote: “Nanowire based electrical sensors for multiplexed detection of
biological/chemical species down to single particle level, and new advances in
nanophotonic sources/detectors for integrated optical-based sensing and/or photon
detection”

7 November 2005 – Fifth Annual Richard M. and Patricia H. Noyes Lectureship,
University of Oregon
“Science and Technology at the Nanoscale”

23 January 2006 – Photonics West 2006, San Jose CA
Keynote: “Nanowire Nanophotonics”

15 February 2006 – MITRE Nanophotonics Workshop, McLean VA
Keynote: “Integrated Nanowire Nanophotonic Systems for Advanced Applications”

Student/Postdoctoral Presentations

February 26, 2003 – Nanotech 2003 Conference, San Francisco, CA
“Silicon-Germanium Epitaxial Core-Shell Nanowire Heterostructure Devices”
(Lincoln Lauhon – contributed talk)

March 5, 2003 – American Physical Society Conference, Austin, TX
“Synthesis and Electrical Characterization of Novel Nanoscale Heterostructures in
Silicon-Germanium Nanowires”
(Lincoln Lauhon – contributed talk)

March 24, 2003 – American Chemical Society Spring Meeting, New Orleans, LA
“Nanowire Nanosensors”
(Wayne Wang – contributed talk)

April 25, 2003 – Materials Research Society Spring Meeting, San Francisco, CA
“Integrated Optoelectronics Assembled from Semiconductor Nanowire Building Blocks”
(Yu Huang – invited paper)

April 26, 2003 – The Fifth Annual Northeast Student Chemistry Research Conference,
Boston University, Boston, MA
“Nanowires as Building Blocks for Nanoscale Science and Technology: Building a Big
Future from Small Things”
(Deli Wang – invited talk)

October 6, 2003 – 4th International Symposium on Atomic Level Characterizations for
New Materials and Devices '03, Kauai, Hawaii
“Characterization of Nanowires for Photonic Devices”
(Carl Barrelet – contributed talk)

October 9, 2003 – 4th International Symposium on Atomic Level Characterizations for
New Materials and Devices '03, Kauai, Hawaii
“Structure Analysis of Molecular Scale Single Crystal Silicon Nanowires”
(Yue Wu – contributed talk)

November 7, 2003 – AVS 50th International Symposium & Exhibition, Baltimore, MD

**“Ultrasensitive Nanowire Sensor for Drug Discovery and Medical Diagnostics”
(Wayne Wang – contributed talk)**

December 1, 2003 – 2003 MRS Fall Meeting, Boston, MA
**“Hierarchical Organization of Nanowires for Integrated Nanoelectronic and Nanophotonic Systems”
(Song Jin – invited talk on behalf of Charles M. Lieber)**

December 2, 2003 – 2003 MRS Fall Meeting, Boston, MA
**“Molecular Scale Single Crystal Silicon Nanowires: Synthesis, Reaction, and Structure Characterization”
(Yue Wu – contributed talk)**

December 4, 2003 – 2003 MRS Fall Meeting, Boston, MA
**“Large-scale Hierarchical Organization of Nanowires for Integrated Arrays of High Performance Semiconductor Nanowire Devices”
(Song Jin)**

December 4, 2003 – MRS Fall Meeting, Boston, MA
**“Nanowire NanoLEDs as Integrated Light Sources for Microfluidic Devices”
(Oliver Hayden – contributed talk)**

December 4, 2003 – MRS Fall Meeting, Boston, MA
**“Branched Semiconductor Nanowires for Nanoelectronics”
(Deli Wang – contributed talk)**

December 4, 2003 – MRS Fall Meeting, Boston, MA
**“Synthesis of Nanowires and Heterostructures for Photonic Devices”
(Carl Barrelet – poster presentation)**

December 4, 2003 – MRS Fall Meeting, Boston, MA
**“Optical Studies of Lasing in Single CdS Nanowires”
(Ritesh Agarwal – poster presentation)**

February 16, 2004 – IEEE Conference on Nanoscale Devices and System Integration, Miami, FL
**“High-performance Nanowire Electronics and Photonics on Glass and Plastic Substrates”
(Michael C. McAlpine – contributed talk)**

March 25, 2004 – APS March Meeting, 2004, Montreal, CA
**“Nanowire-Based Avalanche Photodiodes”
(Ritesh Agarwal – contributed talk)**

March 28, 2004 – 227th ACS National Meeting, Anaheim, CA
**“Optical Studies of the Mechanism of Lasing in Single Cadmium Sulfide Nanowires”
(Ritesh Agarwal – contributed talk)**

April 14, 2004 – 2004 MRS Spring Meeting, San Francisco, CA
“High-Performance Nanowire Electronics and Photonics on Glass and Plastic Substrates”
(Robin Friedman – poster)

April 15, 2004 – 2004 MRS Spring Meeting, San Francisco, CA
“Core-Shell Approach to Complimentary Doping of Semiconductor Nanowires”
(Andrew Greytak – contributed talk)

April 15, 2004 – 2004 MRS Spring Meeting, San Francisco, CA
“Ultrasensitive Nanowire Sensors for Drug Discovery and Medical Diagnostics”
(Wayne Wang – contributed talk)

November 30, 2004 – Materials Research Society 2004 Fall Meeting, Boston, MA
“Synthesis and Characterization of GaN/InGaN/GaN Radial Core/Shell Nanowire Heterostructures ”
(Silvija Gradecak – Contributed Talk)

November 30, 2004 – Materials Research Society 2004 Fall Meeting, Boston, MA
“Branched and Hyper-branched Nanowire Structures as Building Blocks for Nanoelectronics and Nanophotonics ”
(Fang Qian – Contributed Talk)

December 3, 2004 – Materials Research Society 2004 Fall Meeting, Boston, MA
“Gallium Nitride-Based Nanowire Radial Heterostructures for Nanophotonics ”
(Yat Li – Contributed Talk)

14 March 2005 – 229th ACS National Meeting, San Diego, CA
“Nanowire Photonic Circuit Elements”
(Carl Barrelet – Contributed Talk)

22 March 2005 – 2005 APS March Meeting, Los Angeles, CA
“Manipulation and Assembly of Semiconductor Nanowires with Holographic Optical Traps”
(Ritesh Agarwal – Contributed Talk)

23 March 2005 – 2005 APS March Meeting, Los Angeles, CA
“Nanowire Photonic Circuit Elements”
(Andrew Greytak – Contributed Talk)

19 July 2005 – Gordon Research Conference: Chemistry of Electronic Materials,
Connecticut College, New London, CT
“Nanowire Photonic Circuit Elements”
(Carl Barrelet – Poster Presentation)

1 August 2005 – Gordon Research Conference: Clusters, Nanocrystals, and Nanostructures, Connecticut College, New London, CT

"Waveguiding and modulation of light in semiconductor nanowires"

(Andrew Greytak – Poster Presentation)

28 August 2005 – ACS Fall 2005 Meeting, Washington DC

"General synthesis and properties of manganese-doped II-VI and III-V diluted magnetic semiconductor nanowires"

(Pavle Radovanovic – Contributed Talk)

29 August 2005 – ACS Fall 2005 Meeting, Washington DC

"General synthesis and properties of manganese-doped II-VI and III-V diluted magnetic semiconductor nanowires"

(Pavle Radovanovic – Poster Presentation)

30 November 2005 – MRS Fall 2005 Meeting, Boston, MA

"Modulation-Doped Nanowires for Nanoelectronics and Nanophotonics"

(Chen Yang – Contributed Talk)

G. TECHNOLOGY TRANSITIONS STEMMING FROM RESEARCH EFFORT

Research results from the AFOSR funded studies are being transitioned to commercial sector. Specifically, patents results from these studies

- i. C.M. Lieber, Y. Cui, X. Duan, and Y. Huang, "Doped Elongated Semiconductors, Growing Such Semiconductors, Devices Including Such Semiconductors and Fabricating Such Devices", 09/935,776, U.S. patent pending; PCT/US01/26298, International patent pending; EPO 1966109.9 European patent pending; 10-2003-7002636 South Korean patent pending; 90120587 Taiwan patent pending; patents also filed in Singapore, Hong Kong, Mexico, Japan, China, Canada and Australia.
- ii. C.M. Lieber, X. Duan, Y.Cui, Y. Huang, M.S. Gudiksen, L. Lauhon, J. Wang, H. Park, Q. Wei, W. Liang, D.C. Smith, D. Wang, and Z. Zhong, "Nanoscale Wires and Related Devices", 10/196,337 U.S. Patent Pending, 10,720,020 Continuation Pending on 10/196,337, 11/058,443 Continuation Pending on 10,720,020, PCT/US02/16133 International patent application designating Australia Application 2002324426, Canada Application 2,447,728, Japan Application 2003-511316, European Patent Office Application 02759070.2.
- iii. C.M. Lieber, X. Duan, Y. Huang, and R. Agarwal, "Nanoscale Coherent Optical Components", 10/624,135, U.S. patent pending; 10/734,086 U.S. Continuation Patent Pending. US non-provisional and PCT filed Jan 11, 2006.

have been filed by Harvard University, and licenses have been executed with Nanosys, Inc. for the commercial development of this research.

NEW DISCOVERIES, INVENTIONS OR PATENT DISCLOSURES

In addition, a new patent arising from the AFOSR work has been filed by Harvard University:

- iv. C.M. Lieber, C.J. Barrelet, and A.B. Greytak, "Nanowire Photonic Circuits, Components Thereof, and Related Methods", U.S. Provisional Patent Pending 60/592,058.
- v. C.M. Lieber, R. Agarwal, G. Yu, K. Ladavac, and D. Grier, "System and Method for Processing Nanowires with Holographic Optical Tweezers", U.S. Provisional Patent Pending 60/643,384.

H. HONORS AND AWARDS EARNED DURING AWARD PERIOD

Nanotech Briefs Nano 50 Award (2005);

World Technology Award in Materials (2004)

Fellow of the Institute of Physics (2004)

National Academy of Sciences (elected 2004)

ACS Award in the Chemistry of Materials (2004)

Scientific American Award in Nanotechnology and Molecular Electronics (2003)

Nelson W. Taylor Award, Pennsylvania State University (2003);

World Technology Award in Materials (2003)

New York Intellectual Property Law Association Inventor of the Year (2003)

APS McGroddy Prize for New Materials (2003)

Editorial/Advisory

Co-Editor, NanoLetters

Advisory Board, Advances in Nanoscale Materials and Nanotechnology, book series.

Editorial Board, Applied Physics Letters

Advisory Board, Chemical and Engineering News

Editorial Board, Current Nanosciences

Editorial Advisory Board, Encyclopedia of Nanoscience and Nanotechnology

Editorial Advisory Board, Fullerenes, Nanotubes and Carbon Nanostructures
Advisory Board, Institute of Atomic and Molecular Sciences
Member of Advisory Committee, International Academic Advisory Committee
Scientific Advisory Committee, International Society for Nanoscale Science,
Computation and Engineering
Editorial Board, Journal of Applied Physics
Editorial Board, Journal of Computational and Theoretical Nanoscience
Editorial Board, Journal of Nanoscience and Nanotechnology
Editorial Board, Journal of Physical Chemistry
Advisory Editorial Board, Journal of Physics: Condensed Matter.
Editorial Advisory Board, Nanotech Briefs
Advisory Board, Nanotechnology Opportunity Report™
Editorial Advisory Board, Small
Editorial Board, Virtual Journal of Nanoscale Science and Technology, American
Institute of Physics